LARGE DEFORMATION BEHAVIOR OF LOW-ANGLE PIPELINE ELBOWS SUBJECTED TO IN-PLANE BENDING

Koji YOSHIZAKI[1], Masanori HAMADA[2] And Thomas D O'ROURKE[3]

SUMMARY

Substantial permanent ground deformation (PGD) can be generated during earthquakes, causing deformation and strain that concentrates at pipeline elbows. This paper describes in-plane bending experiments that were conducted in the closing and opening mode to evaluate the response of various kinds of low-angle pipeline elbows to earthquake-induced PGD. The experiments involved pipe specimens with 100, 200 and 300-mm diameters and initial bend angles of 45º, 22.5º and 11.25º. In the closing mode, no leakage occurred even when both straight pipes connected to the elbows came into contact and measured maximum strain exceeded 70%. The deformation involved ovalization of the elbows. In contrast, leakage was observed in the opening mode for all cases except the ones that reached the load limit of the hydraulic jack. The strain measured near the crack was 30% in the longitudinal direction. The paper also describes Finite Element (FE) modeling that was performed to simulate the deformation behavior of low-angle pipeline elbows using linear shell elements. There is very good agreement between the analytical and experimental results for plastic deformation exceeding 30% strain.

INTRODUCTION

During earthquakes, permanent ground deformation (PGD) can damage buried pipelines. There is substantial evidence from previous earthquakes, such as the 1983 Nihonkai-Chubu (Japan Gas Association, 1984), the 1994 Northridge (O'Rourke et al., 1996), and the 1995 Hyogoken-Nanbu (Oka, 1996) earthquakes, of gas pipeline damage caused by earthquake-induced PGD in the form of liquefaction and landslides. Because elbows represent locations of local restraint with respect to flexural and axial deformation of buried pipelines, strains can easily accumulate in elbows in response to PGD.

Yoshizaki et al. (1998, 1999) have shown a favorable comparison between the results of in-plane bending experiments with 90º elbows and the analytical results of Finite Element (FE) modeling for strains as high as 25%. In the field, however, many elbows are installed with angles less than 90º, and damage to these facilities has been observed during past earthquakes.

The purpose of this paper is to present experimental results and an analytical method for assessing the behavior of buried pipelines with low-angle elbows subjected to very high levels of strain. In-plane bending experiments were conducted in the closing and opening mode for various kinds of elbows until the measured strain exceeded 30%. Finite Element (FE) modeling was also performed to represent the deformation behavior of the elbows.

BENDING EXPERIMENTS OF LOW-ANGLE ELBOWS

[1] *Visiting Scientist, Cornell University, Ithaca, NY 14853, ky54@cornell.edu*
[2] *Professor, Waseda University, Tokyo, 169-8555, Japan, hamada@mn.waseda.ac.jp*
[3] *Thomas R. Briggs Professor of Engineering, Cornell University, Ithaca, NY 14853, tdo1@cornell.edu*

Experimental Method

In-plane bending experiments were carried out in the closing and opening mode for pipeline elbows with different geometric characteristics. The experiments involved pipe specimens with 100, 200 and 300-mm diameters and initial bend angles of 45º, 22.5º and 11.25º. The radius of curvature was 1.5 times the diameter. The elbows were composed of STPT 370 steel (Japanese Industrial Standard, JIS-G3456), with a specified minimum yield stress of 215 MPa and a minimum ultimate tensile strength of 370 MPa. The straight pipe was composed of SGP steel (JIS-G3452), with a minimum ultimate tensile strength of 294 MPa. The dimensions of the test pipes are presented in Table 1.

Table 1. Summary of Experimental Pipe Dimensions

Nominal diameter (mm)		100	200	300
Elbow	Outside diameter, Do (mm)	116.5	218.4	319.9
	Pipe thickness, t (mm)	5.4	6.8	7.4
	Do/t	21	32	43
Straight pipe	Wall thickness, t (mm)	4.1	5.2	6.5

Figure 1 illustrates the experimental setup. Straight pipes with lengths of about 2.5 times the diameter for 200-mm and 300-mm-diameter pipes and 5 times the diameter for 100-mm-diameter pipes were welded to each end of the test elbows. Displacement was applied with a hydraulic jack in one direction for both the closing and opening mode. Because it has already been confirmed by Minami et al. (1997) and Yoshizaki et al. (1998) that strain rate due to seismic motion has little influence on the stress-strain relationship of gas pipeline steel, the displacement was applied in a quasi-static state. Internal pressure of 0.1 MPa was added with nitrogen. The test was stopped if the both ends of the specimen came into contact with each other in the closing mode, a maximum load of 490 kN was attained, or leakage occurred.

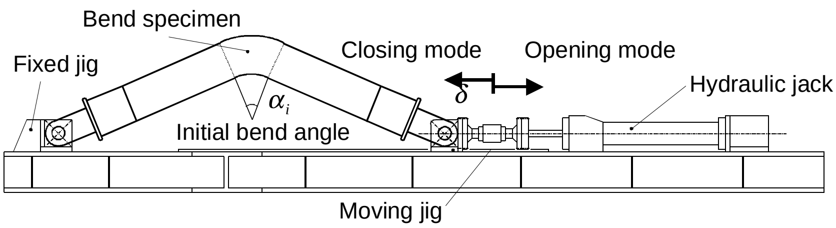

Figure 1 Experimental Setup

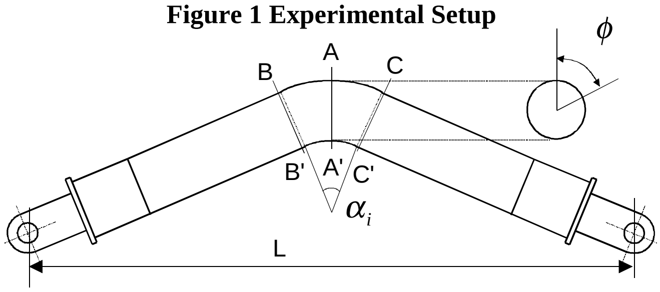

Figure 2 Strain Gauge Locations

Test data were obtained with a load cell, displacement meter, pressure gauge, and strain gauges that were bonded in the circumferential and longitudinal directions on the external pipe surface at the three cross-sections illustrated in Figure 2. As many as 150 strain gauges were used in each test set-up. During each experiment, the gauges, which reached their strain limit of 10%, had to be replaced to continue the acquisition of strain measurements at a given location. In addition, changes in the deformed shape of the A-A' section illustrated in Figure 2 (hereafter, "the central cross-section") were measured intermittently with a 3-dimentional displacement measuring device, employing five arms with five encoders.

Experimental Results and Discussions

Table 2 summarizes the experimental maximum strain, direction of maximum strain, maximum change in bend angle, and observations pertaining to leakage in combination with the results of the previous experiments on 90º elbows (Yoshizaki et al, 1999). In this table, maximum strain means the maximum value of all circumferential and longitudinal strains measured with strain gauges, and is expressed as positive if it is tensile and negative if compressive. For the 100-mm elbow with 22.5º of initial bend angle and the 200-mm elbow with 45º of initial bend angle, maximum strain could not be measured because cracking occurred at a location somewhat distant from the nearest gages. The change in bend angle $\Delta\alpha$ in this table was calculated with the following formula on the assumption that the specimen is a triangle:

$$\Delta\alpha = 2 \cdot \cos^{-1}\left(\frac{L-\delta}{L}\cos\frac{\alpha_i}{2}\right) - \alpha_i \qquad (1)$$

In this formula, L, δ and α_i are the initial distance between the ends of the specimen (illustrated in Figure 2), displacement of the jack, and initial bend angle, respectively.

Table 2 Summary of Test Results

Nominal Diameter			100-mm	200-mm	300-mm
Closing mode	α_i = 90º	Maximum strain	25%, Circum.	30%, Circum.	25%, Circum.
		Max bend angle change, $\Delta\alpha$	78º	86º	81º
		Presence of leakage	No	No	No
	α_i = 45º	Maximum strain	32%, Long.	53%, Long.	43%, Long.
		Max bend angle change, $\Delta\alpha$	119º	118º	113º
		Presence of leakage	No	No	No
	α_i = 22.5º	Maximum strain	57%, Long.	41%, Circum.	72%, Long.
		Max bend angle change, $\Delta\alpha$	133º	134º	134º
		Presence of leakage	No	No	No
	α_i = 11.25º	Maximum strain	58%, Long.	53%, Long.	0.1%, Circum.
		Max bend angle change, $\Delta\alpha$	150º	145º	6º
		Presence of leakage	No	No	(Load limit)
Opening mode	α_i = 90º	Maximum strain	40%, Long.	42%, Long.	33%, Circum.
		Max bend angle change, $\Delta\alpha$	-44º	-33º	-44º
		Presence of leakage	Yes	Yes	(Load limit)
	α_i = 45º	Maximum strain	31%, Long.	22%†, Long.	3%, Circum.
		Max bend angle change, $\Delta\alpha$	-45º‡	-23º	-8º
		Presence of leakage	Yes	Yes	(Load limit)
	α_i = 22.5º	Maximum strain	13%†, Long.	9%, Long.	0.7%, Circum.
		Max bend angle change, $\Delta\alpha$	-22º‡	-10º	-4º
		Presence of leakage	Yes	(Load limit)	(Load limit)
	α_i = 11.25º	Maximum strain	9%, Long.	3%, Long.	—
		Max bend angle change, $\Delta\alpha$	-11º‡	-11º‡	—
		Presence of leakage	(Load limit)	(Load limit)	—

Circum.: Circumferential, Long.: Longitudinal †: Maximum strain could not be measured.
‡: Maximum bend angle change at full extension of elbow (see Figure 2)

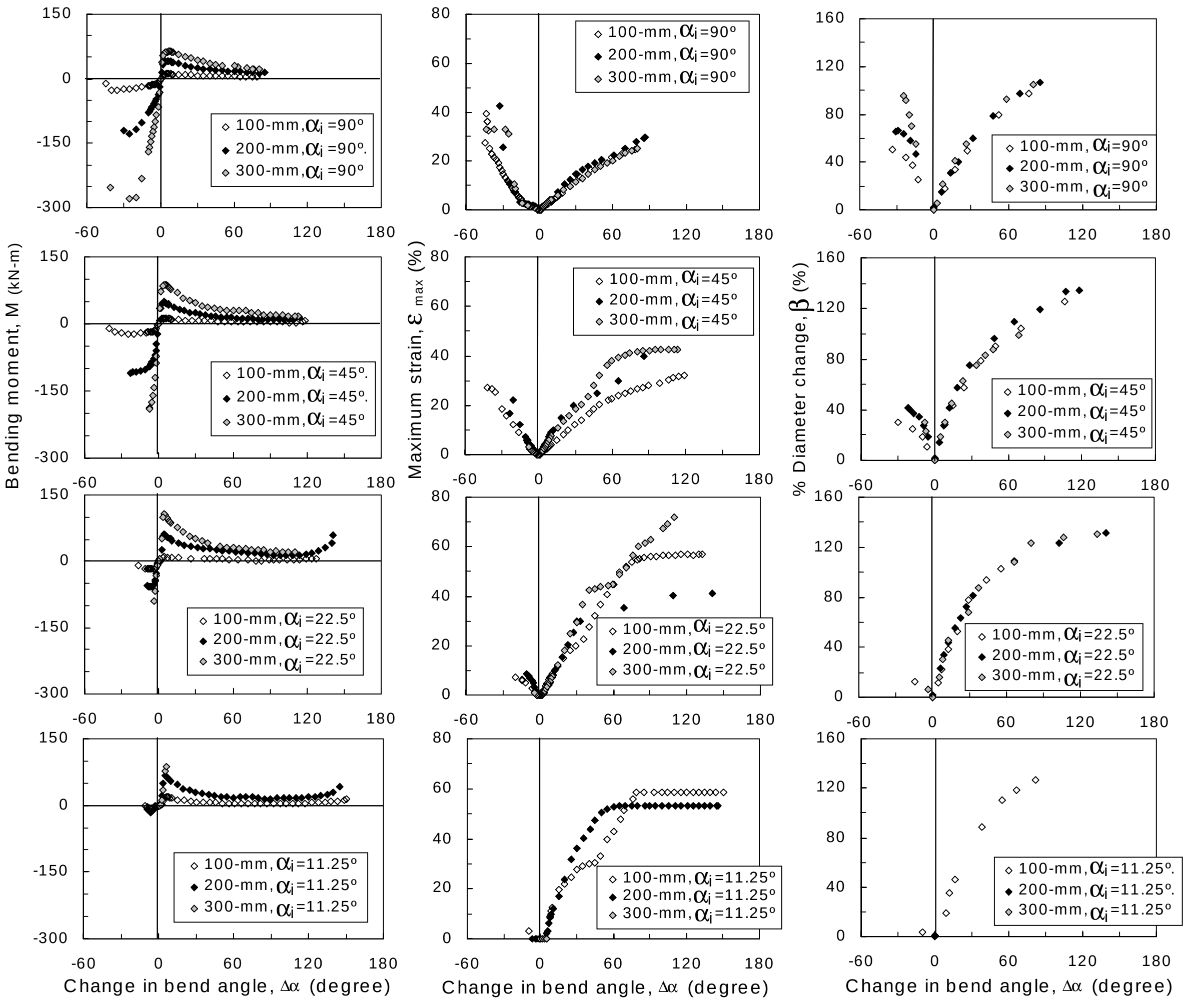

Figure 3 Results of Bending Experiments

Figure 3 is divided into three principal plots showing (a) bending moment, (b) maximum strain, (c) % diameter change vs. change in bend angle. Here, the maximum strain represents the maximum of the absolute values of all measured strains. Bending moment, M, and % diameter change, β, are calculated with the following formulas:

$$M = F \cdot \frac{L-\delta}{2}\sqrt{\frac{L^2}{(L-\delta)^2 \cos\frac{\alpha_i}{2}} - 1} \qquad (2)$$

$$\beta = \frac{D_{\max} - D_{\min}}{\overline{D}_0} \times 100 \qquad (3)$$

In these formulas, F, $D_{\max}$, $D_{\min}$, and $\overline{D}_0$ are, respectively, reaction force measured by a load cell between the jack and the specimen, longest diameter (major axis) of the deformed central cross-section, its shortest diameter (minor axis), and the average of the initial diameter of the undeformed central cross-section.

The deformation behavior was different in the closing and opening mode. In the closing mode, no leakage occurred even when both straight pipes connected to the elbow came into contact with each other and the measured maximum strain exceeded 70%. Elbows with smaller initial bend angles experienced larger changes of bend angle, as indicated in Table 2.

Figure 4 shows the deformation behavior and the deformed shape of the central cross-section of a 300-mm elbow with 22.5º of initial bend angle. The deformation involved ovalization of the elbow. A maximum circumferential tensile strain of 10% was measured when the change in bend angle, $\Delta\alpha$, was 12º (see Figure 4 (a)). Further increases in $\Delta\alpha$ resulted in a shift of maximum strain from circumferential tension to longitudinal compression. A maximum longitudinal compressive strain of 72% was measured at ϕ = 120º (see Figure 2) when $\Delta\alpha$ =134º (see Figure 4 (b)). Because of difficulties in locating and replacing strain gauges at the precise locations of high deformation and curvature, it is likely that the actual maximum strains were larger than those measured with strain gauges and plotted in the figure.

For the pipes, which had same initial bend angle, elbows with larger diameters had larger bending moments for a given change in bend angle, as shown in Figure 3 (a) in the closing mode. Pipe diameter, however, had little effect on the relationships between both maximum strain and % diameter change and changes in the bend angle, as shown in Figure 3 (b) and (c), respectively. For the same diameter pipes, elbows with smaller initial bend angles had larger peak values of moment with larger maximum strains for the same change in bend angle. The main reason for this behavior is that elbows with smaller initial bend angles experience greater localized deformation, which is similar to the buckling behavior of a straight pipe subjected to combined compression and bending.

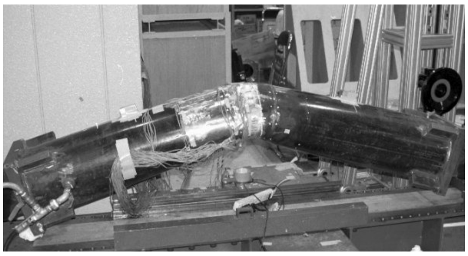


(a) Maximum circumferential strain = 10%, $\Delta\alpha$ = 12º (b) Maximum longitudinal strain = -72%, $\Delta\alpha$ = 134º

Figure 4 Longitudinal and Transverse Deformation of a 300-mm-diameter Elbow with 22.5º of Initial Bend Angle in the Closing Mode

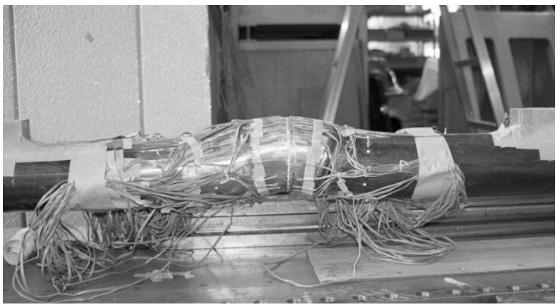
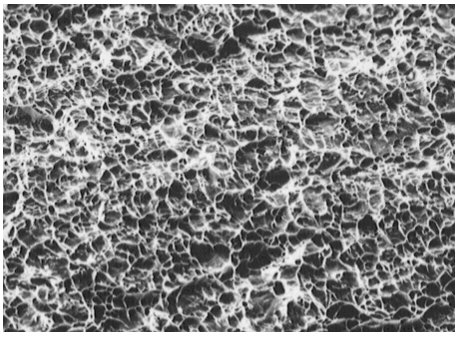

(a) Maximum longitudinal strain = 31%, $\Delta\alpha$ = -42º (b) SEM photograph of the fractured surface

Figure 5 Longitudinal and Transverse Deformation and SEM Photograph of the Fractured Surface of a 100-mm-diameter Elbow with 45º of Initial Bend Angle in the Opening Mode

In contrast, leakage was observed in the opening mode for all cases except the ones at the load limit of the hydraulic jack. Figure 5 shows the deformation behavior and the deformed shape of the central cross-section of a 100-mm elbow with 45º of initial bend angle. In contrast with the closing mode, ovalization during the opening mode was accompanied by increases in vertical diameter at the central cross-section. In response to this change in the central cross-section shape, the stiffness of the elbow became larger than that of the straight pipe. Bending was then concentrated at the location where one of the straight pipes was connected to the elbow. In all cases, leakage occurred near a straight pipe girth weld at ϕ = 180º.

The maximum strains were located near the welds connecting the straight pipes to the elbow. These maximum longitudinal strains are indicated with a photo of the deformed test specimen in Figure 5 (a). The maximum strain measured near the crack was 31% in the longitudinal direction. Necking was observed in the pipe metal outside the heat-affected zone, but close to the crack. Figure 5(b) is a SEM (Scanning Electron Microscope) photograph of the fracture surface of the 100-mm-diameter elbow that indicates a ductile fracture.

Compared with the closing mode, the maximum changes in bend angle were much smaller, as shown in Table 2. For the pipes that had the same initial bend angle, elbows with larger diameters sustained larger bending moments, larger maximum strains, and larger % diameter changes for the same change in bend angle, as shown in Figure 3 (a), (b) and (c), respectively.

FINITE ELEMENT ANALYSES OF LOW-ANGLE ELBOWS

Analytical Model

Finite element analyses were performed to represent the deformation behavior of the low angle elbows. Figure 6 shows the FE model for the 300-mm diameter pipe with 45º of initial bend angle. Because of symmetry, only a quarter of the specimen was modeled, for which half the pipe circumference was analyzed. The elements used in the model are isotropic linear shell elements. Seventy-two elements were employed around half the pipe circumference. As shown in the figure, the density of elements increased near the center of the elbow. The total number of elements was about 7500, of which 4500 were concentrated near the center of the elbow.

The average value of the actual thickness measured with an ultrasonic thickness meter was used in the analytical model. ABAQUS version 5.7 was used as a solver for the analyses with geometric nonlinearity and large strain formulation.

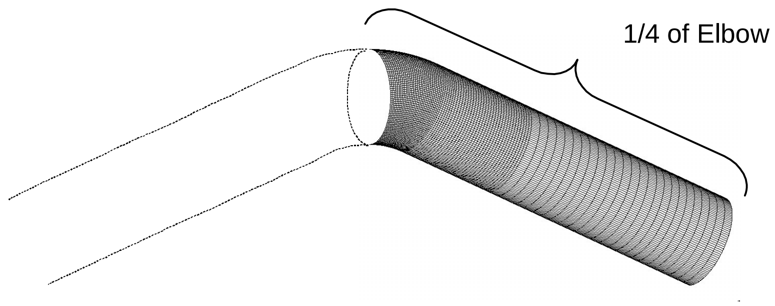

Figure 6 Finite Element Model for 300-mm-diameter Elbow with 45º of Initial Bend Angle

Analytical Results and Discussions

Figure 7 compares the experimental and FE analytical results for the 300-mm elbows with 45º of initial bend angle. Good agreement was observed between the experimental and analytical results with respect to the bending moments and maximum strains plotted in Figure 5. The validity of the numerical modeling technique was confirmed for plastic deformation exceeding 30% strain, as shown in Figure 7 (c). The reason for the difference in maximum compressive strain between the experimental and FE analytical results for changes in bend angle above 60º (see Figure 7 (c)) is related to difficulties in locating and replacing strain gauges at high deformation and curvature. Good agreement between experimental and analytical results was observed for the strain distribution of the central cross-section in the circumferential and longitudinal direction when the change of bend angle, $\Delta\alpha$, was 110º in the closing mode, as shown in Figures 10 (a) and (b), respectively.

Figures 9 (a) and (b) compare the analytical and experimental results for a 100-mm elbow with 45º of initial bend angle when the change in bend angle was -45º in the opening mode. In the experiment, leakage occurred around one of the girth welds between the elbow and the straight pipes. The model represents the strain concentration at the location where leakage occurred in the experiment. As shown in Figure 10, the validity of the model was confirmed for plastic deformation exceeding 30% strain.

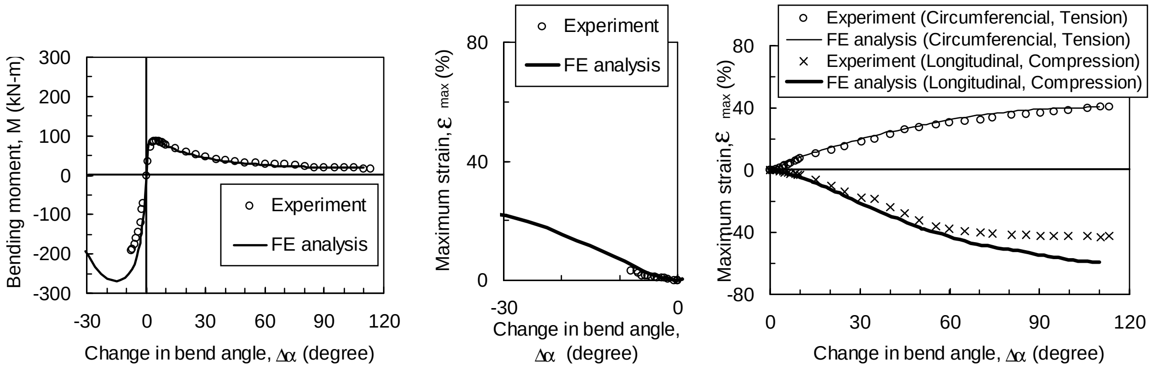

(a) Bending moment (b) Maximum strain (Opening mode) (c) Maximum strain (Closing mode)

Figure 7 Comparison between Experiment and FE analyses for a 300-mm-diameter Elbow with 45º of Initial Bend Angle

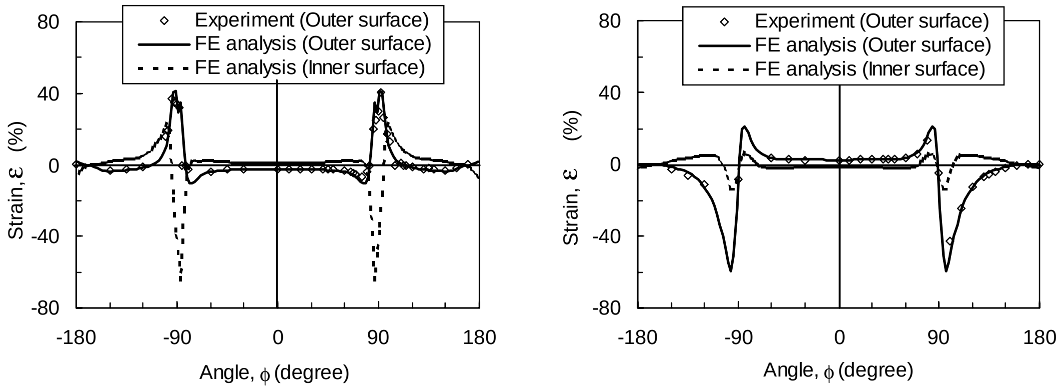

a) Circumferential direction (b) Longitudinal direction

Figure 8 Strain Distribution at the Central Cross-section of a 300-mm-diameter Elbow with 45º of Initial Bend Angle in the Closing Mode ($\Delta\alpha$ = 110º)

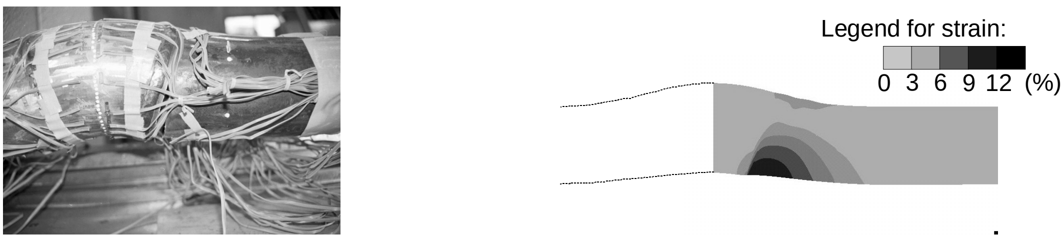

(a) Deformed shape (Experiment) (b) Deformed shape and strain distribution (FE analysis)

Figure 9 Deformed Shape of a 100-mm-diameter Elbow with 45º of Initial Bend Angle in the Opening Mode ($\Delta\alpha$ = -45º)

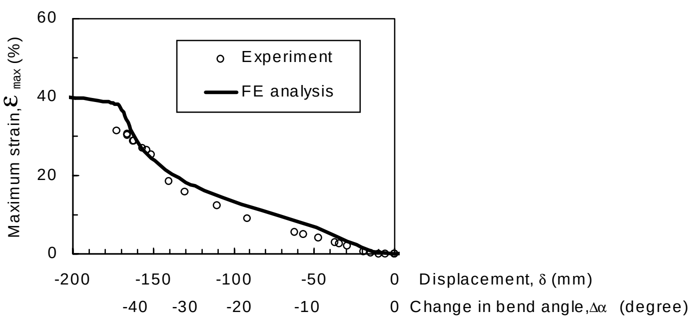

Figure 10 Comparison between Experiment and FE analysis for a 100-mm-diameter Elbow with 45º of Initial Bend Angle in the Opening Mode

CONCLUSIONS

This paper describes in-plane bending experiments that were conducted in the closing and opening mode to evaluate the response of various kinds of low-angle pipeline elbows to earthquake-induced PGD. In the closing mode, no leakage occurred even when both straight pipes connected to the elbows came into contact and measured maximum strain exceeded 70%. The deformation involved ovalization of the elbows. Pipe diameter had little effect on the relationship between maximum strain and bending angle. For the same diameter pipes, elbows with smaller initial bend angles had larger peak values of strain and % diameter change. In contrast, leakage was observed in the opening mode for all cases except the ones that reached the load limit of the hydraulic jack. The strain measured near the crack was 30% in the longitudinal direction. Compared with the closing mode, the maximum changes in bend angle were much smaller in the opening mode. For the same diameter pipes, elbows with smaller initial bend angle had smaller maximum changes in bend angle. For the pipes, which had the same initial bend angle, elbows with larger diameters had larger bending moments, larger maximum strains, and larger % diameter changes for same change in bend angle.

The paper also describes the Finite Element (FE) modeling that was performed to simulate the deformation behavior of the elbows using linear shell elements. There is very good agreement between the analytical and experimental results for plastic deformation exceeding 30% strain.

ACKNOWLEDGEMENTS

The authors wish to thank Mr. Noritake Oguchi, Mr. Hirokazu Ando, Mr. Hiroshi Sugawara, Mr. Naoto Hagiwara, Mr. Hiroshi Yatabe and Mr. Naoyuki Hosokawa of Tokyo Gas for their assistance.

REFERENCES

Japan Gas Association (1984), “Nihonkai-Chubu earthquake and the City Gas”, Japan Gas Association, Tokyo Japan (in Japanese).

Minami, F., Morikawa, J., Ohmasa, M., Toyoda, M., Konda, N., Arimochi, K., Ishikawa, N., Kubo, T. and Shimanuki, H. (1997), “Strength and Fracture Properties of Structural Steels under Dynamic Loading”, *Proceedings*, 16th International Conference on Offshore Mechanics and Arctic Engineering, Yokohama, Japan, Vol.3, pp.283-292.

Ohuchi, H., and Sato, H. (1986), “An Experimental Study on the Large Deformation Behavior of the Pipe-Bend of Buried Pipeline”, *Journal of Structural Engineering*, Tokyo, Japan, Vol.32A, pp.865-878, (in Japanese).

Oka, S (1996), “Damage of Gas Facilities by Great Hanshin Earthquake and Restoration Process”, *Proceedings*,6th Japan-U.S. Workshop on Earthquake Resistant Design of Lifeline Facilities and Countermeasures Against Soil Liquefaction, NCEER-96-0012, Buffalo, NY, pp.111-124.

O’Rourke, T. D. and Palmer, M. C (1996), “Earthquake Performance of Gas Transmission Pipelines”, *Earthquake Spectra*, Vol. 20, No. 3, pp.493-527.

Yoshizaki, K., and Oguchi, N. (1996), “Estimation of the Deformation Behavior of Elbows for an Earthquake-resistant Design”, *Proceedings*, 11th World Conference on Earthquake Engineering, Acapulco, Mexico, Paper No. 1783, Elsevier Science.

Yoshizaki, K. and Oguchi, N. (1998), “Effect of Strain Rate on Stress/Strain Properties of Gas Pipeline Steel”, *Proceedings*, 10th Japan Earthquake Engineering Symposium, Yokohama, Japan, pp. 3171-3174, (in Japanese).

Yoshizaki, K., Hamada, M. and O’Rourke, T. D. (1999), “Large Deformation Behavior of Pipelines with Elbows”, *Proceedings*, 5th U.S. Conference on Lifeline Earthquake Engineering, ASCE, Reston, VA (in press).